frontiers | Frontiers in Energy Research

ORIGINAL RESEARCH
published: 14 April 2022
doi: 10.3389/fenrg.2022.887561

Chaotic Oscillation Control Model of Power System Under Electromechanical Power Disturbance

*Qiankun Hu**

School of Intelligent Manufacturing, Huanghuai University, Zhumadian, China

The influence of electromechanical power on the power system is controlled in order to stabilize the power system. The author establishes a fourth-order power system model with a power disturbance term based on the dissipative property; the possibility of the existence of a system chaotic attractor is analyzed using the Lyapunov exponent spectrum, bifurcation diagram, phase diagram, spectral entropy, etc., and the influence of the power disturbance term on the motion state of the system is studied. It can be seen that under the influence of the disturbance frequency, the system will exhibit sufficient dynamic behavior. The parameters of the power disturbance term are more sensitive to the influence of the system power angle, and when the disturbance amplitude reaches a certain value, the power angle will increase sharply, and eventually the system will become unstable. The experimental results show that when controller parameters c_1 = c_2 = 60 are selected, then$\tau = 0.01$, $\eta = 0.3$, and $\varepsilon = 0.001$. Moreover, when two groups of different control objectives $r = 1.2 + 0.1 \sin(t)$ and $r = 1.2$ are chosen, it can be clearly seen that the power angle δ in the system is very unstable before the controller is connected and the fluctuations are large and irregular, whereas after the controller is added for 150 s, the power angle δ tends to become stable, the fluctuation range becomes small and regular, and the system has almost no chattering. In order to reflect the superiority of the author's control method, under the same parameter conditions, the symbolic function $\theta(s) = \mathrm{sgn}(s)$ is used as a switching function of the controller and the tracking control numerical simulation is carried out for the same control objectives $r = 1.2 + 0.1 \sin(t)$ and $r = 1.2$. The controller that adopts the relay characteristic function $\theta(s) = \frac{s}{s+|\varepsilon|}$ as a switching function has a better control effect and the system is smooth and stable without chattering.

Keywords: electromechanical power, power system, chaotic oscillation, control, model

OPEN ACCESS

Edited by:
Fadi AL-Turjman, Near East University, Cyprus

Reviewed by:
Auwalu Mubarak, Near East University, Cyprus
Min Cai, Xuzhou University of Technology, China
Zhongqiang Zhang, Xuzhou University of Technology, China

Correspondence:
Qiankun Hu
huqiankun@huanghuai.edu.cn

Specialty section:
This article was submitted to Smart Grids, a section of the journal Frontiers in Energy Research

Received: *01 March 2022*
Accepted: *22 March 2022*
Published: *14 April 2022*

Citation:
Hu Q (2022) Chaotic Oscillation Control Model of Power System Under Electromechanical Power Disturbance. Front. Energy Res. 10:887561. doi: 10.3389/fenrg.2022.887561

1 INTRODUCTION

Chaos is the seemingly random motion that occurs in deterministic systems. It is the main direction of nonlinear research and generally exists in all macroscopic and microscopic systems of the universe (Wang et al., 2017). At present, chaos theory has penetrated mathematics, physics, chemistry, electronics, information science, biology, geology, meteorology, and cosmology, as well as economics and human brain science, and almost all natural and humanistic fields such as music, art, and sports. Therefore, the chaos theory has a high theoretical research value and practical

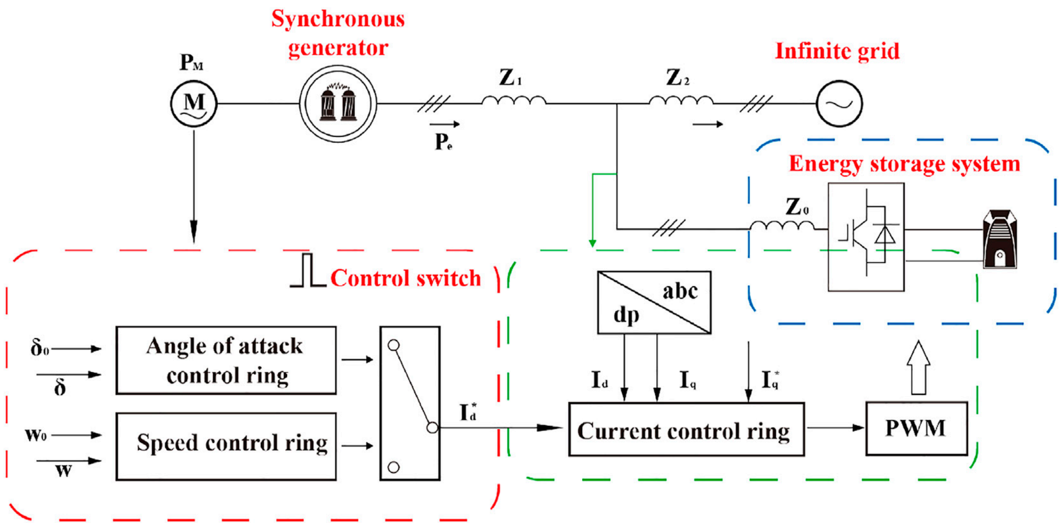

FIGURE 1 | Physical model of power oscillation.

application value (Bi et al., 2016). The power system is a dynamic system with strong coupling, high nonlinearity, and multiple parameters. Its dynamic behavior exhibits many complex nonlinear electromechanical oscillation phenomena. When the system is running normally, it exhibits periodic oscillation (Hou et al., 2021). With the rapid development of large-scale power systems characterized by large units and ultra-high voltage grids, there is a potential threat to the safe operation of the system. Various emergencies and uncertain factors cause continuous and irregular oscillations of the system operating parameters, and chaos often occurs in the actual operation of the power system. In severe cases, the power system may become unstable or even collapse, thereby causing large-scale power outages. The control strategies are aimed at precise integer-order mathematical models, and, in the actual power system, are influenced by external factors and the nature of the system itself. There are uncertainties in system parameters and external disturbances; in particular, new energy and distributed generation are increasingly being introduced into the grid, which further increases the uncertainty of the power system (Wang et al., 2019). These uncertainties easily cause chaotic oscillation of the system and seriously affect the stability of the power system (Zhao and Kamwa, 2020). On the other hand, integer-order systems are approximate idealizations of fractional-order systems. The fractional-order power systems are mainly based on chaotic synchronization. In particular, there is less research on chaos control under uncertain factors, there are not many researches based on chaos control. **Figure 1** shows the physical model of power oscillation. Therefore, for integer-order and fractional-order power system models, considering the influence of internal parameters and uncertain factors of the system, it is necessary to study the chaos control strategy. This will provide the scientific basis and reference data for early warning and processing of the power system's chaotic oscillation. Relative to the relationship between the state variables of the system and input variables, for a linear system that satisfies the superposition principle, the nonlinear system is a kind of irregular motion and is ubiquitous in nature, with the most important motion behavior being the chaotic motion (Preece and Milanovic, 2016). The definition of chaos has not yet reached a consensus in the industry and its expression is complex, with disorder and irregularity; it is often manifested as a nonlinear system under certain conditions and exhibits unpredictable phenomena. It is a manifestation of the fusion of variability and immutability, the presence or absence of sequences or rules. Chaotic motion is neither an invisible phenomenon nor a phenomenon that can be seen by the naked eye. It can be observed only with the help of advanced instruments. It is ubiquitous in the motion state of all things in the universe, and this phenomenon can be observed every day in life (Banerjee et al., 2018; Luo et al., 2020). For example, from the lit blue smoke that suddenly tumbles irregularly after rising and finally dissipates, to the calm stock market that becomes suddenly chaotic because of a stock change, and also the sputtering of water droplets, whose state trajectory is a chaotic phenomenon. Since the 1960s, there have been more and more studies on chaos. It has developed into a very huge discipline system, radiating to physics, economics, finance, meteorology, biology, sociology and other disciplines. At present, the research of various chaos theories will affect the development of modern discipline system, radiation to physics, economics and finance, meteorology, biology, sociology, and other disciplines, and now, every kind of chaos theory research will affect the further development of this modern disciplinary system.

The author proposes a study on the chaotic oscillation control model of the power system under electromechanical power disturbance and establishes a fourth-order power system model with a power disturbance term based on the dissipative property; the possibility of the existence of a system chaotic attractor is analyzed using the Lyapunov exponent spectrum, bifurcation diagram, phase diagram, spectral entropy, etc., and the influence of the power disturbance term on the motion state of the system is studied. It can be seen that under the influence of the disturbance frequency, the system will exhibit sufficient dynamic behavior. The parameters of the power disturbance term are more sensitive to the influence of the system power angle, and when the disturbance amplitude reaches a certain value, the power angle will increase sharply and eventually the system will become unstable.

2 LITERATURE REVIEW

In response to this research problem, Liu et al. (2017) proposed the scientific concept of chaos, which is an important achievement in nonlinear science in recent years. Zhang et al. (2015) proposed a method to calculate the Lyapunov index of a system from a time series, moving chaos research from the theoretical stage to the practical application stage. Errouissi et al. (2017) proposed the OGY control method. Since then, researchers have continued to discover new chaotic systems and hyperchaotic systems, and chaos control has become a new hot spot in chaos research. Besselmann et al. (2016) established a simple power system model and proved that the system will exhibit chaotic oscillation. Mishra et al. (2021) studied in detail the case of considering and ignoring the damping winding, a bifurcation phenomenon in a three-node power system. Since then, the research on chaos control of power system has sprung up. As the world's largest energy producer and consumer, China's goal is the safe and stable operation of power system, which further promotes the in-depth study of power system control theory. Based on a simple interconnected power system model, Shen et al. (2020) analyzed the chaos generation mechanism of a three-parameter system. Zhang et al. (2020) focused on the analysis of its chaotic phenomenon for the classical generator rocking equation. Mousakazemi (2019) studied the chaotic phenomenon of a power system under different instability modes, and, for the first time, two kinds of instability phenomena were found in the ruptured state of the chaotic limit cycle: system angular instability as well as simultaneous voltage and angular instability. Qin et al. (2018) reviewed several bifurcation phenomena in power systems and introduced the application of the chaos theory in short-term load forecasting of power systems. Wang et al. (2020) adopted a nonlinear feedback control method, an active feedback control method, and control research on fractional-order power system chaos. Overbye and Klump (2015) used the fuzzy sliding mode control method to suppress the chaos of the power system and reduce chattering to a certain extent. The authors proposed a study on the chaotic oscillation control model of a power system under electromechanical power disturbance, established a fourth-order power system model with a power disturbance term based on the dissipative property, analyzed the possibility of the existence of a system chaotic attractor using the Lyapunov exponent spectrum, bifurcation diagram, phase diagram, spectral entropy, etc., and studied the influence of the power disturbance term on the motion state of the system, where it can be seen that under the influence of the disturbance frequency, the system will exhibit sufficient dynamic behavior. The parameters of the power disturbance term are more sensitive to the influence of the system power angle, and when the disturbance amplitude reaches a certain value, the power angle will increase sharply and eventually the system will become unstable. The experimental results show that when the controller parameters $c_1 = c_2 = 60$ are selected, then $\tau = 0.01$, $\eta = 0.3$, and $\varepsilon = 0.001$. Moreover, when two groups of different control objectives $r = 1.2 + 0.1\sin(t)$ and $r = 1.2$ are selected, it can be clearly seen that in a system before the controller is connected, the power angle δ is very unstable, the fluctuation range is large, and there is no regularity. However, after the controller is added for 150 s, the power angle δ tends to become stable, the fluctuation range becomes small and regular, and the system has almost no chattering. The system is smooth and stable without chattering.

3 METHODS

3.1 System Modeling

The output voltage E_{fd} of the excitation controller is constrained by the controller, according to the magnitude of the input voltage E_{fdr} that varies within the finite interval $[E_{fd\min}, E_{fd\max}]$, and the system equation can be described as

$$\begin{cases} \dot{\delta} = 2\pi f_0 \omega \\ \dot{\omega} = \dfrac{-d\omega + p_m - \dfrac{E' V_0}{x'_d + x}\sin\delta}{2H} \\ \dot{E}' = \dfrac{-\dfrac{x_d + x}{X'_d + X}E' + \dfrac{x_d - x'_d}{X'_d + X}\cos\delta + E_{fd}}{T'_{d0}} \\ \dot{E}_{fdr} = \dfrac{-K_A\left(V - V_{ref}\right) - \left(E_{fdr} - E_{fd0}\right)}{T_A} \end{cases}. \tag{1}$$

In the above equation, δ is the power angle of the generator, ω is the angular frequency of the generator, f_0 is the fundamental frequency of the synchronous motor, M is the inertia of the generator rotor, d is the damping factor, p_m is the generator of the input power, p_G is delivered by the electromagnetic power of the generator, x is the reactance of the transmission line, x_d is the reactance of the generator, x'_d is the transient reactance of the generator, T'_{d0} is the time constant of the generator stator winding, E_{fd} is the excitation voltage, V_0 is the infinite voltage, and V is the terminal voltage of the generator and can be expressed as

$$V = \frac{1}{x + x'_d}\sqrt{\left(x'_d + xE'\cos\delta\right)^2 + \left(xE'\sin\delta\right)^2}. \tag{2}$$

In the power system, the excitation link of the terminal amplitude limiting method is generally used to protect the equipment of the system, and the output voltage E_{fd} of the excitation controller is expressed as

TABLE 1 | System parameter values.

Parameter name	Numerical value
Synchronous motor fundamental frequency (f_0)	60
Transmission line reactance (X)	0.4
Generator dynamic reactance (x_d)	1
Excitation limiter voltage reference (E_{fd0})	2
Equivalent moment of inertia (h)	4.9
Generator transient reactance (x'_d)	0.4
Bus voltage reference (V_{ref})	1.05
Excitation limiter voltage minimum ($E_{fd\min}$)	0
Infinite bus voltage (V_0)	1
Generator stator time constant (T'_{d0})	10
Excitation time constant (T_A)	1
Excitation limiter voltage max. ($E_{fd\max}$)	5

$$E_{fd} = \begin{cases} E_{fd\max}, E_{fdr} > E_{fd\max} \\ E_{fdr}, E_{fd\min} \le E_{fdr} \le E_{fd\max} \\ E_{fd\min}, E_{fdr} < E_{fd\min} \end{cases}. \tag{3}$$

When the input voltage E_{fdr} is in the interval $[E_{fd\min}, E_{fd\max}]$, the output voltage $E_{fd} = E_{fdr}$ (Ramanathan and Vittal, 2015), and when E_{fdr} exceeds the output upper limit (or lower limit), the output voltage E_{fd} remains at the upper limit $E_{fd\max}$ (or lower limit $E_{fd\min}$) and no longer changes with E_{fdr}, until E_{fdr} returns to the range of the interval $[E_{fd\min}, E_{fd\max}]$ (Liu et al., 2016).

The parameter values are shown in **Table 1**. The dissipation characteristics of Equation (1) can be calculated as shown in Equation (4):

$$\nabla V = \frac{\partial\dot{\delta}}{\partial\delta} + \frac{\partial\dot{\omega}}{\partial\omega} + \frac{\partial\dot{E}'}{\partial E'} + \frac{\partial\dot{E}_{fdr}}{\partial E_{fdr}} = -\frac{d}{2H} - \frac{\frac{x_d + x}{x'_d + x}}{T'_{d0}} - \frac{1}{T_A} = -\frac{d}{10} - \frac{7}{6}. \tag{4}$$

Corresponding to time *t, V* is always shrinking during the movement, as shown in Equation (5). This shows the possibility of the existence of chaotic attractors in the system.

$$V(t) = V(0)e^{-\left(\frac{d}{10}+\frac{7}{6}\right)t}. \tag{5}$$

At the same time, by substituting the system parameter values in **Table 1**, the algebraic equation shown in **Equation 6** can be obtained (Stankovic et al., 2015).

$$\begin{cases} 0 = 120\pi\omega \\ 0 = \dfrac{-d\omega + p_m - \dfrac{E'}{0.4+0.5}\sin\delta}{10} \\ 0 = \dfrac{-\dfrac{1+0.5}{0.4+0.5}E' + \dfrac{1-0.4}{0.4+0.5}\cos\delta + E_{fd}}{10} \\ 0 = -K_a(v - 1.05) - \left(E_{fdr} - 2\right) \end{cases}. \tag{6}$$

Among these, the output voltage E_{fd} is expressed as

$$E_{fd} = \begin{cases} 5, E_{fdr} > 5 \\ E_{fdr}, 0 \le E_{fdr} \le 5 \\ 0, E_{fdr} < 0 \end{cases}. \tag{7}$$

The voltage V is expressed as

$$V = \frac{1}{0.5+0.4} \cdot \sqrt{\left(0.4 + 0.5E'\cos\delta\right)^2 + \left(0.5E'\sin\delta\right)^2}. \tag{8}$$

By setting a set of system parameters $d = 0.5$, $p_m = 1.3$, and$K_A = 150$, and substituting them into Equation (6) for iterative calculation, a set of equilibrium points can be obtained: $(\delta, \omega, E', E_{fdr}) = (1.0409, 0, 1.3559, 1.9229)$.

$$\begin{cases} \dot{\delta} = 2\pi f_0\omega \\ \dot{\omega} = \dfrac{1}{2H}\left(-d\omega + p_m - \dfrac{E'V_0}{x'_d + x}\sin\delta - p_e\cos(2\pi f_1 t)\sin\delta + p_k\cos(2\pi f_2 t)\right) \\ \dot{E}' = \dfrac{-\dfrac{x_d + x}{x'_d + x}E' + \dfrac{x_d - x'_d}{x'_d + x}\cos\delta + E_{fd}}{T'_{d0}} \\ \dot{E}_{fdr} = \dfrac{-K_A\left(V - V_{ref}\right) - \left(E_{fdr} - E_{fd0}\right)}{T_A} \end{cases}. \tag{9}$$

To set the simulated environment parameters, system parameters $D = 2$, $P_m = 1.2$, $K_a = 190$ and the disturbance term parameters $p_e = 0.2$, $f_1 = 0.2$, $p_k = 0$, $f_2 = 0$ are selected; at this time, the system behaves in a state of random chaotic oscillation. In order to suppress the chaotic oscillation phenomenon, a controller to observe the control effect after the system runs for 150 s is added. Here, the controller parameters $c_1 = c_2 = 60$, $\tau = 0.01$, $\eta = 0.3$, and $\varepsilon = 0.001$ are selected. Then, two groups of different control objectives $r = 1.2 + 0.1\sin(t)$ and $r = 1.2$ are chosen to control the effect.

3.2 Influence of the Power Disturbance Term on the System

We will substitute $(\delta, \omega, E', E_{fdr}) = (1.0409, 0, 1.3559, 1.9229)$ as the initial value of the system into **Equation 9** for iterative operation (Silva et al., 2017). Using the bifurcation diagram, Lyapunov exponent spectrum, and phase diagram, the effects of these four parameters on the evolution process of the state attractor of the system are shown respectively (Silva et al., 2017).

3.2.1 Disturbance Amplitude p_e

The presence of the electromagnetic disturbance term may cause the system to appear ultra-high voltage, which affects the stable operations of the system, therefore it is necessary to study the electromagnetic disturbance term. When $p_k = 0$, $f_2 = 0Hz$, and $f_1 = 0.2Hz$ are selected and when $p_e \in (0, 0.2255)$, the p_e bifurcation diagram and Lyapunov exponent spectrum of the system are obtained (Alam et al., 2020).

When $p_e \in (0, 0.1256)$, the two largest Lyapunov exponents (LEs) of the system within the parameter range are kept close to 0 at the same time, that is, the distribution of the LE value of the system in this range is (0,0,-,-,-) by the LE value and the bifurcation diagram. The specific value of LE at the boundary point $p_e = 0.1256$ of the quasi-periodic state and the chaotic state of the system is

TABLE 2 | LE and system status at different p_e values.

p_e	LE	System operating status
0.1237	(0,0,–0.0646,–0.2723,–1.0364)	Quasi-period
0.2250	(0.07620,–0.0217,–0.2882,–0.570)	Chaos

TABLE 3 | LE and system states at different f_1 values.

f_1	LE	System operating status
0.4200	(0,–0.0469,–0.0491,–0.2336,–1.0371)	Cycle
0.8000	(0.0838,0,–0.0329,–0.2612.–1.1564)	Chaos
0.8500	(0,–0.0517,–0.1310,–0.1389,–1.0451)	Cycle
0.9000	(0.0773,0,–0.0196–0.2138,–1.2107)	Chaos
1.2680	(0,–0.0266,–0.1972,–0.2050,–0.9380)	Cycle

(0,0,–0.0944,–0.2502,–1.1088). When p_e continues to increase beyond 0.1256, the maximum LE of the system will also increase rapidly and becomes greater than 0, and the system motion realizes the transition process from quasi-periodic to chaotic. In the range of $p_e \in (0.1256, 0.2255)$, the maximum LE of the system is greater than 0; combined with the bifurcation diagram, it can be seen that the system is running in a chaotic motion state (Dong et al., 2018). **Equation 9** cannot be in a stable state for a long time and causes voltage collapse under excessive disturbance. **Table 2** gives the LE and operating states of the system for some p_e values.

3.2.2 Electromagnetic Disturbance Frequency f_1

Frequency, another important parameter of power disturbance, will also directly affect the motion state of the power system. Without considering the load disturbance and choosing in the range of $f_1 \in (0.7780,0.8205) \cup (0.8740,0.9315)$, the maximum LE is greater than 0, indicating that the system is moving in a chaotic state. When $f_1 \in (0,0.7780) \cup (0.9315,2)$, both the largest and second-largest LEs of the system tend to 0, and it can be seen from the bifurcation diagram that the system is in a quasi-periodic motion state at this time. The change in the motion state of the system from periodic to chaotic corresponds to the above analysis. The corresponding system LEs and operating states of some f_1 values are shown in **Table 3**.

3.2.3 Load Disturbance Amplitude p_k

The presence of load disturbances may cause problems such as harmonics and voltage fluctuations that impair power quality and threaten the stability of the power system; therefore, it is necessary to study the load disturbance term. Without considering the electromagnetic disturbance, $p_e = 0$, $f_1 = 0$, and $f_2 = 0.2$ are selected. The bifurcation graph and Lyapunov exponent spectrum of the system are obtained with respect to p_k when $p_k \in (0,0.2555)$. In the range of $p_k \in (0, 0.1370)$, both the maximum LE and the second-largest LE of the system are close to 0 and the system is now in a quasi-periodic motion state. When $p_k \in (0.1370, 0.2055)$, the maximum LE of the system remains 0, the next largest LE is less than or equal to 0, and the system runs in a periodic state and the number of cycles is large; however, when p_e is changed in the above, no trace of periodic motion is found. When $p_k \in (0.2055,0.2555)$, the maximum LE of the system within the parameter range is obviously positive; at this time, the motion state of the system is in a typical chaotic state. And when the p_k value exceeds 0.2555, the system will collapse due to the phenomenon of power angle divergence due to excessive disturbance. **Table 4** shows the LE and operating states of the system for some p_k values.

TABLE 4 | LE and system status at different p_k values.

p_k	LE	State of motion
0.0903	(0,0,–0.1003,–0.2182,–1.0739)	Quasi-period
0.1703	(0,–0.0628,–0.1287,–0.2227,–0.9660)	Cycle
0.2180	(02167,0,–0.1242,–0.2461,–1.0505)	Chaos

TABLE 5 | LE and system status at different f_2 values.

f_2	LE	Operating status
0.5000	(0,0,–0.0686,–0.4534,–0.8472)	Quasi-period
0.7500	(0,–0.0620,–0.0724,–0.1066,–1.1257)	Cycle
0.8000	(0.0637,0,–0.0274,–0.2505,–1.1525)	Chaos
0.8500	(0,–0.1122,–0.1144,–0.1686,–0.9716)	Cycle
0.9000	(0.1004,0,–0.0281,–0.2503,–1.1887)	Chaos
1.2700	(0,–0.1305,–0.1636,–0.1679,–0.9047)	Cycle

3.2.4 Load Disturbance Frequency f_2

Similar to the above analysis method, without considering electromagnetic disturbance, $p_k = 0.02$, $p_e = O$, and $f_1 = 0$ are chosen, and the bifurcation graph and Lyapunov exponent spectrum of the system are obtained with respect to f_2 when $f_2 \in (0,2)$.

When compared to the situation of changing A, changing B brings about similar changes to the system and there are only a few minor differences. When f_2 is in the range of (0.7615, 0.8130) ∪ (0.8855, 0.9575), the maximum LE of the system is greater than 0, which shows that the motion state of the system is chaotic. When $f_2 \in (0.7135,0.7615) \cup (0.8130,0.8855) \cup (1.2565,1.2775) \cup (1.6820,1.7040)$, the maximum LE of the system is 0 and the rest of the LEs are obviously less than 0; when $f_2 \in (0,0.7135) \cup (0.9575,1.2565) \cup (1.2775,1.6820) \cup (1.7040,2)$, the two largest LE values in the system approach 0 at the same time, which means that the system operates in a quasi-periodic state within this parameter range. From the phase diagrams of the system at f_2 = 0.75 and f_2 = 0.90, it can be clearly seen that the motion state of the system changes from periodic to chaotic, corresponding to the above analysis. The corresponding system LEs and operating states of some f_2 values are shown in **Table 5**.

4 RESULTS AND ANALYSIS

The system parameters D = 2, $P_m = 1.2$, and $K_a = 190$ and the disturbance term parameters $p_e = 0.2$, $f_1 = 0.2$, and $p_k = 0$, $f_2 = 0$ are selected; at this time, the system behaves in a state of random

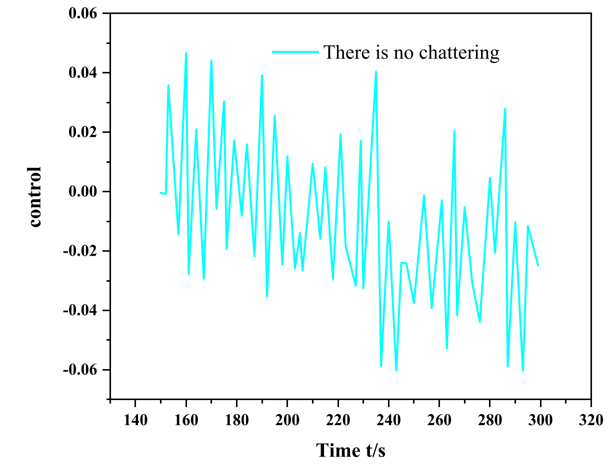

FIGURE 2 | Sliding mode control with target trajectory $r = 1.2 + 0.1\ \sin(t)$.

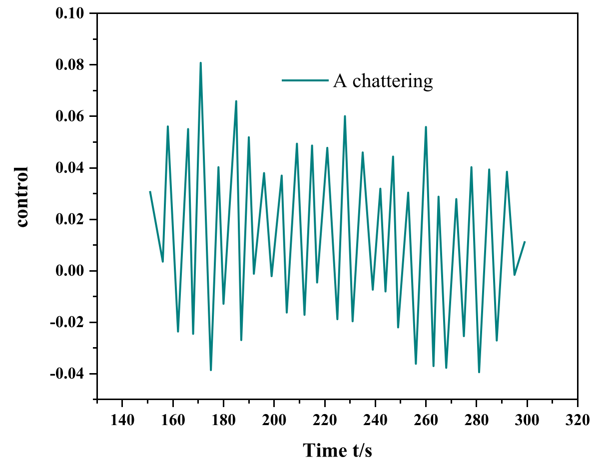

FIGURE 4 | Sliding mode control of target trajectory $r = 1.2 + 0.1\ \sin(t)$ using a sign function.

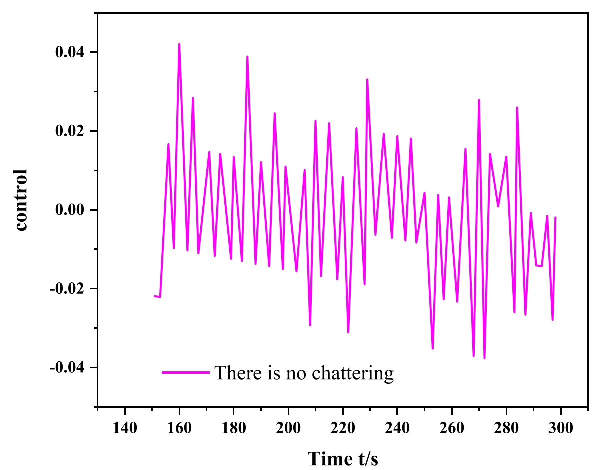

FIGURE 3 | Sliding mode control with target trajectory $r = 1.2$.

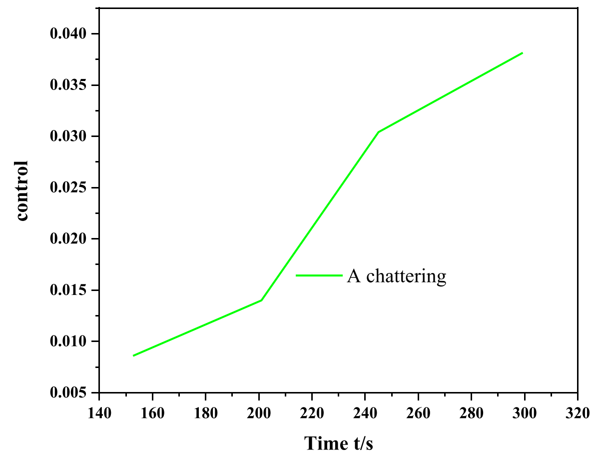

FIGURE 5 | Sliding mode control with a sign function for the target trajectory $r = 1.2$.

chaotic oscillation. In order to suppress the chaotic oscillation phenomenon, a controller to observe the control effect after the system runs for 150 s is added. Here, the controller parameter $c_1 = c_2 = 60$, with $\tau = 0.01$, $\eta = 0.3$, and $\varepsilon = 0.001$, is selected. Choosing two groups of the different control objectives r = 1.2 + 0.1 sin(t) and r = 1.2 controls the effect. The results are shown in **Figures 2**, **3**. It can be clearly seen that the power angle δ in the system is very unstable before the controller is connected, the fluctuations are large and irregular, and after adding the controller for 150 s, the power angle δ tends to become stable, the fluctuation range becomes small and regular, and the system has almost no chattering.

The symbolic function $\theta(s) = \mathrm{sgn}(s)$ with the tracking control numerical simulation is carried out for the same control objectives r = 1.2 + 0.1 sin(t) and $r = 1.2$, and the simulation results are shown in **Figure 4** and **Figure 5**, respectively. Obviously, the controller using the relay characteristic function $\theta(s) = \frac{s}{s+|\varepsilon|}$ as the switching function has a better controlling effect and the system is smooth and stable without chattering. While using the conventional sign function as the switching function, although a good control effect can be obtained, the system chattering is obvious and the chattering frequency is high; at the same time, due to the severe chattering phenomenon, the numerical simulation takes a long time and the amount of data is large.

5 CONCLUSION

This article proposes a chaotic oscillation control model of the power system under electromechanical power interference.

The author proposes a study on the chaotic oscillation control model of a power system under electromechanical power disturbance. By establishing a fourth-order power system model with a power disturbance term, the Lyapunov exponent, bifurcation diagram, and spectral entropy are analyzed and the influence of the power disturbance term on the motion state of the power system is discussed. The simulation results show that the controller can quickly and smoothly suppress the chaotic oscillation of the system, and at the same time, it can effectively avoid the chattering problem and has strong robustness. Chaos control is one of the frontiers of nonlinear research, and the systematization and control methods of the chaos theory still need to be improved. Second, the majority of researchers should consider the engineering realization of chaos control. A large number of simulation experiments have theoretically proved the effectiveness of the control strategy but there is still a certain distance from being widely used in engineering applications. Therefore, researchers have to conduct in-depth research and engineering experiments and use interdisciplinary research methods for referencing to form practical research results.

DATA AVAILABILITY STATEMENT

The original contributions presented in the study are included in the article/Supplementary Material, and further inquiries can be directed to the corresponding author.

AUTHOR CONTRIBUTIONS

The author confirms being the sole contributor to this work and has approved it for publication.

REFERENCES

Alam, M. R., Bai, F., Yan, R., and Saha, T. K. (2020). Classification and Visualization of Power Quality Disturbance-Events Using Space Vector Ellipse in Complex Plane. *IEEE Trans. Power Deliv.* 36 (99), 1. doi:10.1109/TPWRD.2020.3008003

Banerjee, A., Chaudhuri, N. R., and Kavasseri, R. G. (2018). A Novel Explicit Disturbance Model-Based Robust Damping of Inter-area Oscillations through Mtdc Grids Embedded in Ac Systems. *IEEE Trans. Power Deliv.* 33, 1. doi:10.1109/tpwrd.2018.2799170

Besselmann, T. J., Almér, S., and Ferreau, H. J. (2016). Model Predictive Control of Load-Commutated Inverter-Fed Synchronous Machines. *IEEE Trans. Power Electro.* 31 (10), 7384–7393. doi:10.1109/TPEL.2015.2511095

Bi, T., Qin, J., Yan, Y., Liu, H., and Martin, K. E. (2016). Disturbance Propagation Mechanism Based on the Electromechanical Wave Theory. *IET Generation, Transm. Distribution* 10 (12), 2891–2898. doi:10.1049/iet-gtd.2015.1268

Dong, K., Shi, T., Xiao, S., Li, X., and Xia, C. (2018). A Finite Set Model Predictive Control Method for Quasi-Z Source Inverter-Permanent Magnet Synchronous Motor Drive System. *IET Electric Power Appl.* 13 (3), 302–309.

Errouissi, R., Al-Durra, A., Muyeen, S. M., and Leng, S. (2017). Continuous-time Model Predictive Control of a Permanent Magnet Synchronous Motor Drive with Disturbance Decoupling. *Iet Electric Power Appl.* 11 (5), 697–706. doi:10.1049/iet-epa.2016.0499

Hou, G., Ke, Y., and Huang, C. (2021). A Flexible Constant Power Generation Scheme for Photovoltaic System by Error-Based Active Disturbance Rejection Control and Perturb & Observe. *Energy* 237 (9), 121646. doi:10.1016/j.energy.2021.121646

Liu, H., Loh, P. C., Wang, X., Yang, Y., Wang, W., and Xu, D. (2016). Droop Control with Improved Disturbance Adaption for a Pv System with Two Power Conversion Stages. *IEEE Trans. Ind. Electron.* 63 (10), 6073–6085. doi:10.1109/tie.2016.2580525

Liu, Z., Miao, S., Fan, Z., and Han, J. (2017). Markovian Switching Model and Non-linear DC Modulation Control of AC/DC Power System. *IET Generation, Transm. Distribution* 11 (10), 2654–2663. doi:10.1049/iet-gtd.2016.1862

Luo, S., Lewis, F. L., Song, Y., and Ouakad, H. M. (2020). Accelerated Adaptive Fuzzy Optimal Control of Three Coupled Fractional-Order Chaotic Electromechanical Transducers. *IEEE Trans. Fuzzy Syst.* 29 (99), 1. doi:10.1109/TFUZZ.2020.2984998

Mishra, D., Singh, B., and Panigrahi, B. K. (2021). Adaptive Current Control for a Bidirectional Interleaved Ev Charger with Disturbance Rejection. *IEEE Trans. Industry Appl.* 57 (99), 1. doi:10.1109/tia.2021.3074612

Mousakazemi, S. M. H. (2019). Control of a Pwr Nuclear Reactor Core Power Using Scheduled Pid Controller with ga, Based on Two-point Kinetics Model and Adaptive Disturbance Rejection System. *Ann. Nucl. Energ.* 129 (JUL), 487–502. doi:10.1016/j.anucene.2019.02.019

Overbye, T. J., and Klump, R. P. (2015). Determination of Emergency Power System Voltage Control Actions. *IEEE Trans. Power Syst.* 13 (1), 205–210. doi:10.1109/59.651637

Preece, R., and Milanovic, J. V. (2016). Efficient Estimation of the Probability of Small-Disturbance Instability of Large Uncertain Power Systems. *IEEE Trans. Power Syst.* 31 (2), 1063–1072. doi:10.1109/tpwrs.2015.2417204

Qin, J., Bi, T., Liu, H., and Martin, K. E. (2018). Model Approach of Power Networks Based on Unsymmetrical Inertia Distribution for Disturbance Propagation Study. *IET Generation, Transm. Distribution* 12 (9), 2055–2064. doi:10.1049/iet-gtd.2017.1243

Ramanathan, B., and Vittal, V. (2015). Small-disturbance Angle Stability Enhancement through Direct Load Control Part Ii-Numerical Simulations and Results. *IEEE Trans. Power Syst.* 21 (2), 782–790. doi:10.1109/TPWRS.2006.873025

Shen, J., Li, W. D., Liu, L., Jin, C., and Wang, X. (2020). Frequency Response Model and its Closed-form Solution of Two-Machine Equivalent Power System. *IEEE Trans. Power Syst.* 36 (99), 1. doi:10.1109/TPWRS.2020.3037695

Silva, L. R. M., Kapisch, E. B., Martins, C. H. N., Filho, L. M. A., Cerqueira, A. S., Duque, C. A., et al. (2017). Gapless Power-Quality Disturbance Recorder. *IEEE Trans. Power Deliv.* 32 (2), 862–871. doi:10.1109/tpwrd.2016.2557280

Stankovic, A. M., Dukic, S. D., and Saric, A. T. (2015). Approximate Bisimulation-Based Reduction of Power System Dynamic Models. *IEEE Trans. Power Syst.* 30 (3), 1252–1260. doi:10.1109/tpwrs.2014.2342504

Wang, D., Ma, N., and Guo, C. (2017). Characteristics of Electromechanical Disturbance Propagation in Non-uniform Power Systems. *IET Generation, Transm. Distribution* 11 (8), 1919–1925. doi:10.1049/iet-gtd.2016.1126

Wang, F., He, L., and Rodriguez, J. (2020). Fpga-based Continuous Control Set Model Predictive Current Control for Pmsm System Using Multistep Error Tracking Technique. *IEEE Trans. Power Electron.* 35 (12), 13455–13464. doi:10.1109/tpel.2020.2984336

Wang, L., Liang, H. R., Prokhorov, A. V., Mokhlis, H., and Huat, C. K. (2019). Modal Control Design of Damping Controllers for Thyristor-Controlled Series Capacitor to Stabilize Common-Mode Torsional Oscillations of a Series-Capacitor Compensated Power System. *IEEE Trans. Industry Appl.* 55, 1. doi:10.1109/tia.2019.2892343

Zhang, R., Xu, Y., Dong, Z. Y., and Wong, K. P. (2015). Post-disturbance Transient Stability Assessment of Power Systems by a Self-adaptive Intelligent System. *IET Generation, Transm. Distribution* 9 (3), 296–305. doi:10.1049/iet-gtd.2014.0264

Zhang, Y., Jiang, T., and Jiao., J. (2020). Model-free Predictive Current Control of Dfig Based on an Extended State Observer under Unbalanced and Distorted Grid. *IEEE Trans. Power Electron.* 35 (8), 8130–8139. doi:10.1109/tpel.2020.2967172

Zhao, J., and Kamwa, I. (2020). Guest Editorial: Next Generation of Synchrophasor-Based Power System Monitoring, Operation and Control. *IET Generation Transm. Distribution* 14 (19), 3943–3944. doi:10.1049/iet-gtd.2020.1315

Conflict of Interest: The author declares that the research was conducted in the absence of any commercial or financial relationships that could be construed as a potential conflict of interest.

Publisher's Note: All claims expressed in this article are solely those of the authors and do not necessarily represent those of their affiliated organizations, or those of the publisher, the editors, and the reviewers. Any product that may be evaluated in this article, or claim that may be made by its manufacturer, is not guaranteed or endorsed by the publisher.

Copyright © 2022 Hu. This is an open-access article distributed under the terms of the Creative Commons Attribution License (CC BY). The use, distribution or reproduction in other forums is permitted, provided the original author(s) and the copyright owner(s) are credited and that the original publication in this journal is cited, in accordance with accepted academic practice. No use, distribution or reproduction is permitted which does not comply with these terms.